LINKING HYPERSPECTRAL IMAGERY AND FOREST INVENTORIES FOR FOREST ASSESSMENT IN THE CENTRAL APPALACHIANS

Jane R. Foster and Philip A. Townsend[†]

ABSTRACT.—Hyperspectral imagery from EO-1 Hyperion and AVIRIS were used in conjunction with continuous forest inventory (CFI) data to map detailed forest composition in the state forests of Western Maryland. We developed a hierarchical vegetation classification that conformed to the National Vegetation Classification Standard (NVCS) at the Alliance level and mapped these forest types as a function of hyperspectral reflectance using decision trees. Overall classification accuracy for vegetation at the Alliance level was very high (60-80 percent), with field validation indicating accuracies ranging from 65-70 percent. In an area dominated by oaks, the hyperspectral imagery was able to accurately distinguish plots dominated by individual red oaks with acceptable success (>60 percent). Hyperspectral imagery also differentiated between conifers more than 70 percent of the time. Overall, the accuracies were improved over similar analyses conducted using multi-date Landsat data. Our research demonstrates the capacity for hyperspectral imagery to remotely monitor, map and model forest systems in the Central Appalachians. The resulting forest composition maps can inform forest management decisions with a level of information content not previously available.

Mapping forest types is one of the primary applications of remote sensing data to forest management. In the past, standard satellite imagery available from Landsat era sensors has been limited in its ability to differentiate between specific hardwood forest types such as those described at the Alliance level of the National Vegetation Classification Standard (NVCS) (http://biology.usgs.gov/npsveg/nvcs.html). Forest maps with species level detail continue to be desired by forest managers and scientists alike, yet remain difficult to produce from satellite imagery without complex methods, extra data sources, and intense time and effort. Hyperspectral imagery improves upon the limits of Landsat data by measuring the reflectance of light in more than two hundred narrow bands, compared to Landsat TM's seven wide bands. Specific portions of the hyperspectral spectrum have been linked to forest indicators such as forest stress measured by canopy chlorophyll content (Sampson et al. 2003) and the biophysical content of leaves (Townsend et al. 2003, Smith et al. 2003). As such, the high data content found in hyperspectral data promises to greatly enhance forest mapping capabilities when used in conjunction with typical forest inventory data. We tested the ability of hyperspectral imagery from two sensors combined with Continuous Forest Inventory (CFI) data to map forest composition to the Alliance level and compared the results to a similar classification created from multi-season Landsat TM data.

Study Area

Green Ridge State Forest (GRSF) is a 16,000 ha working forest in Western Maryland (fig. 1). It is located in the Ridge and Valley physiographic province of the central Appalachian Mountains, and is characterized by steep northeast to southwest trending mountains, with many deep valleys. Elevation ranges from 200-700 m. Green Ridge lies in the rainshadow of the Allegany front, receiving only 91 cm of rainfall annually, the lowest amount in Maryland. Most of the soils at GRSF are derived from either shale or sandstone with a relatively low water holding capacity (Mash 1996). The forests were largely cleared around the turn of the twentieth century, and are now mostly intact and mature. Scattered clearcuts and deferred harvest cuts at various stages of regrowth are located within the study area, though fewer than 100 ha are typically harvested annually. Large areas of uneven forest are located in places where gypsy moth defoliation over two decades has caused substantial tree mortality. Forests are comprised largely of deciduous oaks, with Virginia

[†]Faculty Research Associate (JRF), University of Maryland Center for Environmental Sciences, Appalachian Laboratory, 301 Braddock Rd., Frostburg, MD 21532; and Associate Professor (PAT), same facility. JRF is corresponding author: to contact, call (301) 689-7127 or e-mail at jfoster@al.umces.edu.

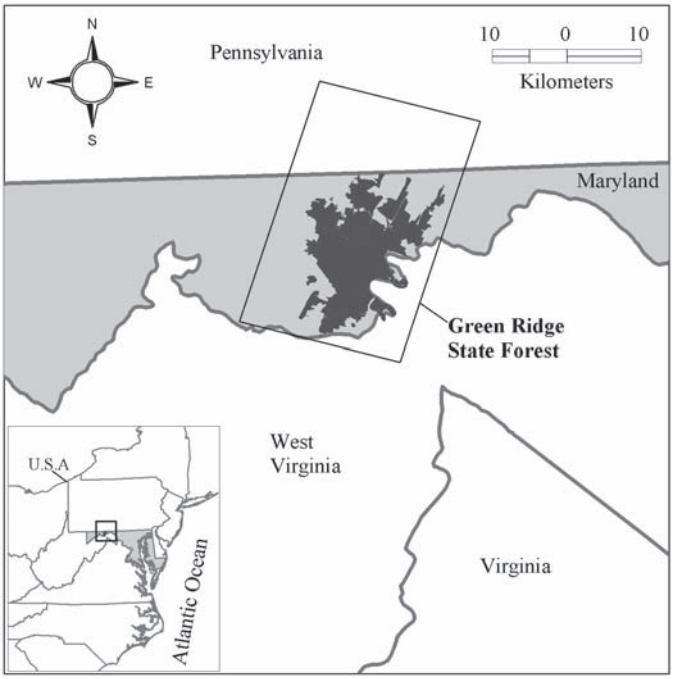

Figure 1.—Location of Green Ridge State Forest, Maryland.

pine (*Pinus virginiana*) and white pine (*Pinus strobus*) mixing in or forming pure stands and hemlock (*Tsuga canadensis*) growing on protected north-facing slopes. Of the key oak species, white oak (*Quercus alba*) and scarlet oak (*Quercus coccinea*) are both prominent on mesic slopes and at lower elevations. Red oak (*Quercus rubra*) and chestnut oak (*Quercus prinus*) are abundant on ridge tops and rocky slopes, and black oak (*Quercus velutina*) dominates mostly on mesic lower slopes. The understory is largely open, although blueberry (*Vaccinium spp*.) can be locally abundant and greenbriar (*Smilax spp.)* frequently expands in Gypsy moth defoliated areas.

Methods

Field Data

Continuous Forest Inventory (CFI) data from the Maryland Department of Natural Resources was used to sample the image data to classify forest types based on image spectra. The CFI database includes 432 plots in GRSF, all of which were sampled in 2000 or 2001. Each CFI plot is a 0.08 ha circular area on which all trees > 12 cm diameter are identified and measured. The CFI plots are arrayed on a regular grid at approximately 550 m intervals, yielding a statistical sample of the population of forest properties within the study area. All plots were geographically referenced using a Trimble Pro XR GPS.

Image Data

Hyperspectral images from sensors on two separate platforms were acquired for this research. A summer Hyperion image was acquired from the EO-1 satellite on 24 July 2001. An AVIRIS image was collected from an ER-2 aircraft on 14 May 2000. Hyperion has a spatial resolution of 30 m and covers a swath 7.68 km wide. It measures 210 bands at approximately 10 nm intervals from 400 nm to 2500 nm. High altitude AVIRIS pixels have approximately 17 m spatial resolution and 224 bands at 10 nm intervals between 400-2500 nm. Hyperion and AVIRIS images were converted to reflectance and referenced to UTM map coordinates as described in Townsend et al. (2003). The Hyperion image was also corrected for terrain illumination effects while the AVIRIS data used for this study was not (Townsend and Foster 2002). Four reflectance spectra were extracted from the hyperspectral images for each CFI plot. These spectral "bundles" were linked without averaging to their respective CFI plot data to create the hierarchical classification trees we used to map forest alliances. 423 plots overlapped with the AVIRIS image area and 283 plots overlapped with the narrower Hyperion image.

Table 1.—Forest associations found at GRSF. (Shaded classes were not validated in the field for this study and are not discussed in the results).

Class #	Class Name	Common Names	N (CFI Plots)
1	*Quercus rubra*	Red Oak	11
3	*Quercus rubra - Quercus spp. - Carya*	Red Oak - Oak species - Hickories	32
4	*Pinus virginiana*	Virginia Pine	36
5	*Pinus virginiana / deciduous mix*	Virginia Pine / Deciduous Mix	23
6	*Quercus prinus - Quercus coccinea*	Chestnut Oak - Scarlet Oak	7
7	*Quercus coccinea* / mix	Scarlet Oak / Mix	35
8	*Pinus rigida*	Pitch Pine	4
9	*Quercus velutina* / mix	Black Oak / Mix	52
10	*Quercus alba*	White Oak	75
11	*Quercus prinus - Quercus* spp. / mix	Chestnut Oak - Oak species / Mix	53
12	*Quercus prinus - Acer rubrum* / mix	Chestnut Oak - Red Maple / Mix	2
14	*Quercus prinus*	Chestnut Oak	21
15	*Prunus serotina*	Black Cherry	3
25	*Fraxinus* spp.	Ash species	1
33	*Sassafras albidum*	Sassafras	2
40	*Robinia pseudoacacia* / mix	Black Locust / Mix	3
42	*Fraxinus americana* / mix	White Ash / Mix	6
43	*Carya* sp.	Hickory species	14
44	*Acer saccharum / Quercus rubra*	Sugar Maple / Red Oak	6
45	*Tilia americana / Acer saccharum*	American Linden / Sugar Maple	1
49	*Pinus strobus*	White Pine	6
50	*Pinus strobus / Quercus* mix	White Pine / Oak Mix	24
52	*Tsuga canadensis*	Eastern Hemlock	5
53	*Liriodendron tulipifera*	Tulip Poplar	2
54	*Liriodendron tulipifera* / mix	Tulip Poplar / Mix	1
55	*Acer saccharum*	Sugar Maple	1
56	*Acer saccharum / Fagus - Fraxinus* mix	Sugar Maple / Beech - Ash Mix	5
59	*Acer rubrum / Fagus - Acer saccharum* mix	Red Maple / Beech - Sugar Maple Mix	1
TOTAL			432

A time-series of Landsat TM images from three dates was used to test the ability of multi-temporal Landsat data to map forest alliances. The time-series included an early spring image from 16 April 1997, an early summer image from 31 May 1996, and a mid-summer image from 24 July 2001. Each Landsat image was converted to planetary reflectance, orthorectified to UTM map coordinates, and corrected for terrain illumination effects using a Cosine correction (Meyer et al. 1993, Allen 2000). Both Landsat and Hyperion images were spatially accurate to within 30 m. Reflectance from TM bands 1-5 and 7 for each date for a total of 18 bands were extracted as described above and put into the CART analysis. 426 CFI plots overlapped with the TM image area.

Vegetation Classification

Vegetation types were assigned based upon the clustering of floristic data from 15,033 forest samples from the Central Appalachian region acquired from several sources, including data we have collected (3,813 plots), samples from the USFS Forest Inventory and Analysis (FIA) database (10,140 plots), and from the CFI database (1,080 plots). Sample areas and number of trees tallied were comparable among datasets, which permitted merging the data from multiple sources. Once the data sets were assembled, species names were standardized and relative basal area was computed by species by plot. The data were clustered using Ward's hierarchical agglomerative method (Lance and Williams 1967), with a small proportion of the plots eliminated as outliers. The classification yielded 41 forest alliances, of which 28 occurred in the Green Ridge study area (table 1). Subsequent to developing the vegetation classification, the image spectra

extracted for each of the CFI plots in GRSF were used to develop target hyperspectral signatures for the 28 associations. The spectral data were then used with decision trees to develop stand type maps.

Statistical Methods

We used classification and regression trees (CART) to map the Alliance level forest classes from spectral signature bundles. A variety of approaches have been used to map forest composition with hyperspectral data in mountainous landscapes (Martin et al. 1998) and with mixed forests (van Aardt and Wynne 2001). CART is being used increasingly for mapping from remotely sensed imagery (Friedl and Brodley 1997, Friedl et al. 1999, Hess et al. 1995, Cairns 2001) and is only generally described here. Classification trees – also known as decision trees – are fitted by binary recursive partitioning, in which data sets are consecutively divided into smaller subsets with increasing statistical homogeneity (Clark and Pregibon 1993). CART approaches are desirable because they are less sensitive to non-linearities in the input data than methods that require assumptions of Gaussian distributions (as do many image classification techniques) (Clark and Pregibon 1993, Venables and Ripley 1994). In addition, CART is an extremely valuable approach for data exploration when a very large set of independent predictor variables are available, e.g. with hyperspectral data sets. CART does not require data reduction, tests for normality or data transformations. One limitation to CART is that its performance is most robust and repeatable with large data sets, such as the CFI vegetation database that we used.

Field Validation

Forest maps created from the CART classification were validated using the "fuzzy sets" methodology originally proposed by Gopal and Woodcock (1994, also Townsend and Walsh 2001). Traditional measures of accuracy assessment that report simple "yes-no" accuracy are limited in applicability to complex forest landscapes because they assume all locations on a map can be unambiguously mapped to a single category. In addition, traditional methods do not convey the degree of error or mismatch between mapped categories and actual composition. Forest communities in the Appalachians are naturally heterogeneous and highly variable, grading across types in terms of both species dominance and presence. For this reason, forest composition can be described as "fuzzy," and it can be acknowledged that for any one location it either may be difficult to identify any single best community type label or, alternatively, a location may be reasonably classified into two or more types. For example, in this work, we attempt to map forests dominated by black, red and scarlet oaks, whereas in many locations forests contain a mix of the three species. To accommodate this, in an accuracy assessment using fuzzy sets, all validation locations are assigned a fuzzy membership rating in all possible classes (from 1, completely wrong, to 5, absolutely right); fuzzy membership scores are then used to assess the magnitude and sources of confusion and ambiguity in the classification. We report 3 assessments of accuracy using the method of Gopal and Woodcock (1994): (1) percent accuracy for mapping to the "best" class vs. mapping to an "acceptable, but not necessarily the best" class), (2) the mean magnitude of errors by class, and (3) the source of errors (the average number of classes with acceptable membership for a given class).

NVC standards suggest visiting a minimum of 10 sites for each class when validating forest vegetation maps. Using an AVIRIS classification as a base map, we selected 10 validation sites for each class that was represented by more than 10 plots in the CFI plot data, for a total of 11 classes (see un-shaded classes in table 1). These sites were distributed widely and were generally accessible from forest roads. Incidental validation plots were added to replace inaccessible plots or when a unique forest type was observed. These plots increased the number of validated forest alliances to 15. Expert assessment was conducted independent of knowledge of the classification. We visited a total of 146 validation plots. Because of slight differences in the three maps from different sensors, the number of validation sites per forest type varies based on the map being analyzed.

Results

The results of the accuracy assessment of CART classification maps from each sensor are summarized in Tables 2 and 3, and require some explanation for those unfamiliar with fuzzy assessments. Table 2 shows different accuracy measures for all the field validated forest types. The learning accuracy for the CART classification trees is shown in the LEARN column and represents the percentage of the CFI forest plots

used to create the classification tree that were mapped to the correct class by that tree. According to learning accuracy, AVIRIS predicted CFI forest plot type with 80.9 percent accuracy overall, followed by Hyperion (64.4 percent) and Landsat (62 percent). AVIRIS mapped 10 of the 15 most abundant classes with a learning accuracy greater than 75 percent, of which 4 pine classes and the white oak class exceeded 90 percent accuracy. In comparison, Hyperion mapped only 5 classes with learning accuracy near or greater than 75 percent. These forest types included Virginia pine, white oak, black oak mix, white pine/deciduous mix and eastern hemlock. Landsat TM had the lowest overall learning accuracy, mapping only 4 forest types well (> 75 percent).

The remaining columns in Table 2 show the results of the fuzzy set analysis designed to measure the frequency of matches and mismatches between the mapped forest types and the independent validation data. The number of samples (N) corresponds to the number of validation sites visited for each class for a particular map. We include two accuracy metrics from the fuzzy set analysis in this table. The MAX metric represents the percentage of validation sites that were mapped to the absolute best class as seen in the field. The RIGHT metric represents the percentage of validation sites that were mapped to a good or acceptable forest type. This measure gives a better sense of map accuracy for the map user, because it illustrates the probability that a point on the map will be mapped to a class that agrees to a large extent with what is observed on the ground. The improvement in accuracy gained from the MAX to the RIGHT metric is shown in the IMP column. We can see that the RIGHT function improved the MAX accuracy by 20-25 percent on average.

According to MAX total, all three forest vegetation maps have a low overall validation accuracy ranging from 41.3 percent for Landsat to 46.5 percent for Hyperion. Fortunately, the RIGHT measure shows that the actual ability of the classifications to map good or acceptable classes ranges from 65.3 percent for Hyperion to 70.2 percent for AVIRIS. Hemlock stands, which are easy to distinguish both spectrally and in the field, were mapped to the best possible class with consistently high accuracy by each sensor. The forest type that was mapped with a relatively high RIGHT accuracy most consistently across platforms was the black oak mix class with 79.2 percent success for AVIRIS, 68 percent (Hyperion), and 82.1 percent (Landsat). AVIRIS mapped 9 out of 12 validated classes with 60 percent accuracy or greater. Hyperion mapped 7 out of 11 validated classes with 60 percent accuracy or greater and Landsat TM broke 60 percent accuracy with 7 out of 12 validated classes. Considering the degree of mixing among the forest vegetation classes being mapped, these accuracy levels are a promising accomplishment. No previous studies have attempted to map such specific classes.

Table 3 illustrates the average magnitude and direction of the map validation errors (MAG) and the average fuzzy membership statistic (MEMBER). Where a mismatch occurs between the best forest type in the field and the actual forest type found on the map, the MAG statistic shows the average difference between the maximum score given for a forest type at a given site and the next highest score given for other possible forest types. For example, a site mapped as chestnut oak – oak species / mix turned out to actually fit the exact description of the chestnut oak – scarlet oak class when visited in the field. In this case, the maximum score given was a 5 to the chestnut oak – scarlet oak class and the second highest score was a 4 for the chestnut oak – oak species / mix class. The difference value for this particular site would be the score for the mapped forest type (4) minus the maximum score (5) resulting in a value of –1. A case where a site is accurately mapped as the best possible class with no other reasonable choices would give a difference of 5-1, or +4. A MAG value of zero indicates that a site was accurately mapped to the best possible class. Thus MAG values close to zero are desirable. Slightly negative values show that although the best class was not correctly mapped for that site, it was actually mapped to the next best choice. Given the specificity and mixing characteristic of our forest alliances, we did not expect to find many cases where there were strongly positive differences except for very distinct classes such as the hemlock, which had slightly positive MAG values for AVIRIS and Hyperion.

The average difference values for each sensor hover around a value of –1 with AVIRIS having the least negative difference, indicating that when the best forest type was not matched by the map, the mapped class had a score only 1 unit below the best. This result confirms that our forest types are generally not distinct classes with discrete boundaries, but rather mixes dominated by sets of species that vary

Table 2.—Results of classification learning accuracy and fuzzy set field validation accuracy metrics for three sensors

	AVIRIS					EO-1 HYPERION					LANDSAT TM				
Class Name	N	LEARN	MAX	RIGHT	IMP	N	LEARN	MAX	RIGHT	IMP	N	LEARN	MAX	RIGHT	IMP
Quercus rubra		43.0%				2	30.0%	100.0%	100.0%	0.0%	7	34%	71.4%	71.4%	0.0%
Quercus rubra - Quercus spp. - *Carya* mix	5	66.0%	20.0%	60.0%	40.0%	11	53.0%	36.4%	81.8%	45.5%	5	16%	40.0%	80.0%	40.0%
Pinus virginiana	13	95.0%	38.5%	76.9%	38.5%	18	95.0%	38.9%	55.6%	16.7%	18	99%	44.4%	66.7%	22.2%
Pinus virginiana / deciduous mix		93.0%					68.2%				3	78%	0.0%	33.3%	33.3%
Quercus prinus - Quercus coccinea	1	46.0%	0.0%	0.0%	0.0%		0.0%					0%			
Quercus coccinea / mix	13	77.0%	30.8%	69.2%	38.5%	6	51.0%	33.3%	66.7%	33.3%	9	32%	11.1%	55.6%	44.4%
Pinus rigida	3	94.0%	0.0%	33.3%	33.3%		0.0%					0%			
Quercus velutina / mix	24	85.0%	58.3%	79.2%	20.8%	25	74.0%	56.0%	68.0%	12.0%	28	69%	50.0%	82.1%	32.1%
Quercus alba	20	93.0%	50.0%	65.0%	15.0%	25	79.0%	44.0%	60.0%	16.0%	22	77%	54.5%	68.2%	13.6%
Quercus prinus - Quercus spp. / mix	12	83.0%	16.7%	58.3%	41.7%	1	49.0%	0.0%	0.0%	0.0%	13	71%	7.7%	46.2%	38.5%
Quercus prinus	7	81.0%	42.9%	85.7%	42.9%		22.0%				3	30%	33.3%	33.3%	0.0%
Carya sp.		64.0%				1	58.3%	0.0%	0.0%	0.0%		59%			
Pinus strobus	7	69.0%	57.1%	71.4%	14.3%	4	30.0%	50.0%	100.0%	50.0%	1	64%	100.0%	100.0%	0.0%
Pinus strobus / *Quercus mix*	5	91.0%	60.0%	80.0%	20.0%	1	88.8%	0.0%	0.0%	0.0%	5	82%	20.0%	60.0%	40.0%
Tsuga canadensis	11	75.0%	72.7%	72.7%	0.0%	7	77.0%	71.4%	71.4%	0.0%	7	36%	57.1%	57.1%	0.0%
TOTAL	121	80.9%	44.6%	70.2%	25.6%	101	64.4%	46.5%	65.3%	18.8%	121	62%	41.3%	66.1%	24.8%

Table 3.—Fuzzy set validation statistics showing the magnitude and direction of errors (MAG) and the average membership per class (MEMBER).

	AVIRIS			EO-1			Landsat TM		
Class Name	N	MAG	MEMBER	N	MAG	MEMBER	N	MAG	MEMBER
Quercus rubra				2	0.00	8.00	7	-0.71	5.00
Quercus rubra - Quercus spp. - Carya mix	5	-1.40	4.60	11	-1.09	5.36	5	-0.80	6.20
Pinus virginiana	13	-0.92	5.62	18	-1.56	5.00	18	-1.28	5.00
Pinus virginiana / deciduous mix							3	-3.00	2.00
Quercus prinus - Quercus coccinea	1	-4.00	6.00						
Quercus coccinea / mix	13	-1.38	5.62	6	-1.50	5.67	9	-2.22	5.56
Pinus rigida	3	-2.33	1.00						
Quercus velutina / mix	24	-0.75	6.34	25	-0.92	5.72	28	-0.93	5.89
Quercus alba	20	-1.00	4.20	25	-1.28	5.08	22	-1.05	4.91
Quercus prinus - Quercus spp. / mix	12	-1.83	5.67	1	-2.00	4.00	13	-2.62	5.85
Quercus prinus	7	-1.00	5.71				3	-2.67	5.33
Carya sp.				1	-4.00	3.00			
Pinus strobus	7	-0.57	4.29	4	-0.25	3.00	1	1.00	2.00
Pinus strobus / Quercus mix	5	-1.00	6.00	1	-4.00	6.00	5	-2.00	4.80
Tsuga canadensis	11	0.27	3.00	7	0.14	3.86	7	-0.71	3.86
TOTAL	121	-1.00	5.09	101	-1.13	5.16	121	-1.37	5.21

compositionally across the landscape. Most individual classes validated by more than 5 sites had difference magnitudes close to -1.

We also include an average membership statistic in Table 3 that indicates the degree of fuzziness for each forest type as mapped by the three different sensors. The MEMBER column shows the average number of classes – including the mapped class – that were potentially acceptable choices for a given site (for example, classes 4 and 5 in Table 1 are both dominated by Virginia pine and it is reasonable to assume that each could potentially be misclassified as the other). A class with high average membership values has a fuzzier distinction from other classes than a class with a relatively low membership value. Most of our forest alliances had an average membership ranging from 4-6 classes. The lowest membership was found in the eastern hemlock class. Of the oaks, the white oak alliance was the most distinct, having the lowest average membership.

Figure 2 shows the forest type map derived from the CART classification tree of AVIRIS data for Green Ridge State Forest. GRSF is bounded on the east by the meandering Potomac River and on the west by a smaller creek, and it is bisected in its northern half by the interstate. Non-forest areas have been masked out in black. Conifers and conifer/deciduous mixes are shown in shades of green, white oak is shown in light blue, and red oak and red oak mix are shown in shades of red. Black oak mix is shown in brown, scarlet oak mix in maroon, and chestnut oak and its mixes in shades of yellow and orange. Rare classes that have not been discussed here are shown in other colors.

The classification map itself can inform us about its ability to predict the distribution of forest associations at the Alliance level. A few characteristics of this particular map suggest that it is in fact mapping these forest classes with reasonable success before even considering the accuracy assessment. First, related mixed forest types tend to occur adjacent to each other or as mixes. This is especially evident with the red oak (Class 1) and red oak – oak species – hickory mix class (Class 3). Where relatively large contiguous patches of red oak dominated forests occur, they almost always occur next to or mixed with the red oak mix class. The same can be said of chestnut oak and its mixes, shown by shades of yellow and orange. In addition, the classes which are mixes of pines and deciduous species often occur as transition zones between the pine dominated forest types and the deciduous forest types. These patterns are expected based on the knowledge of how forest composition changes across species and environmental gradients. Finally, there is a distinct

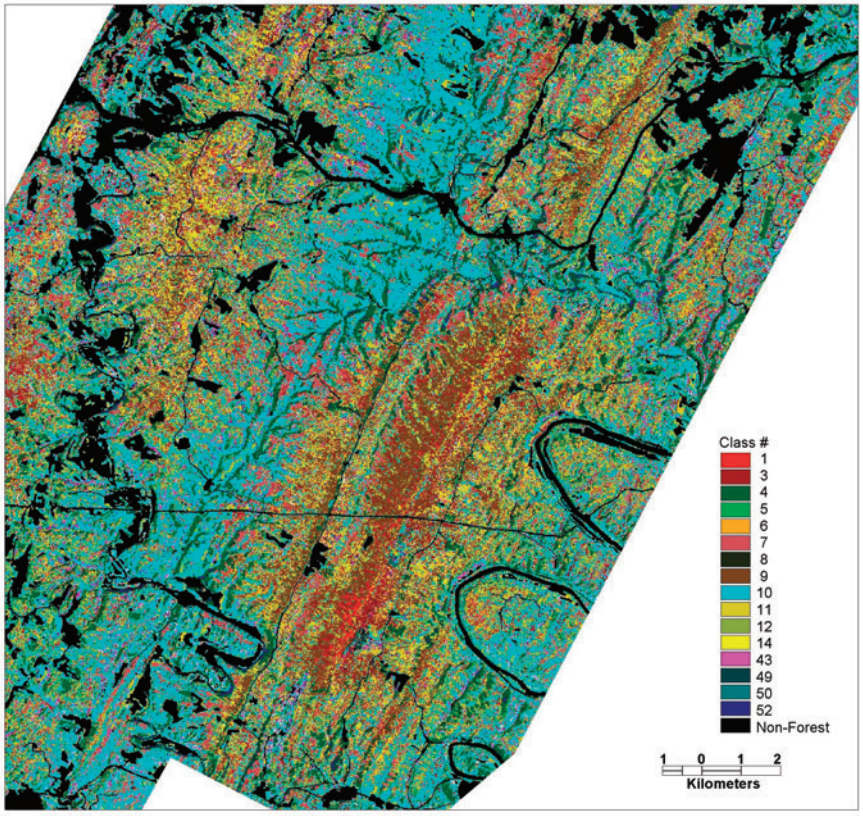

Figure 2.—Map of forest alliances derived from CART classification of AVIRIS imagery. Only the field validated alliances are referenced in the classification key.

dominance of white oak (light blue) in an oblong area running through the center of the state forest that is characterized by a shale substrate and more complex valley and drainage patterns than the rest of the area. In comparison, red oak classes in reds, browns, and yellows tend to dominate the long and linear sandstone mountains oriented northeast to southwest. These two distinct regions represent geological differences that seem to favor the dominance of either red oaks or white oaks.

Discussion

Using CART classification of hyperspectral and forest inventory data, we have produced Alliance level forest maps with accuracies unattainable from traditional methods. In the past, mapping of forest alliances from remotely sensed data typically resulted in accuracies of 40 percent or less (Czaplewski 2003). Our accuracies for maps from AVIRIS data averaged 80 percent for most alliances, which is a substantial increase in accuracy from past efforts. These successes are especially notable considering the various types of uncertainty confronted during this study.

One perplexing result was that white oak was not validated with greater accuracy. This is surprising because it is the most abundant species represented in the CFI data and generally easy to identify in the field. One possible reason for this discrepancy is that the ubiquity of the white oak class across parts of GRSF affects the expert evaluation during the field validation. More than any other class of hardwoods, the white oak class at Green Ridge is dominated by its namesake, with 26 of the 75 white oak CFI plots having a white oak relative basal area of 40 percent or greater. When a large percentage of validation sites sample these relatively pure white oak forests, oak mixes with less conspicuous dominance of white oak may suffer by comparison and subsequently be scored higher as some other type of oak mix. This tendency suggests that the most abundant classes are also characterized by an extreme range of dominance levels and may in fact be more vulnerable to incorrect scoring during fuzzy validation. If this is the case, then the high learning accuracies reported for the white oak forest alliance (93 percent AVIRIS, 79 percent Hyperion, and 77 percent Landsat) are probably closer to the true accuracy than the fuzzy validation values.

The somewhat low MAX accuracy values seen in Table 2 illustrate the difficulty of accurately mapping mixed deciduous forest alliances to the best possible class using hyperspectral data. Revisiting the descriptions of these forest classes in Table 1 underlines this. Several of the most abundant forest types are oak or pine mixes where the dominant species in the type frequently comprises from 30-40 percent of the basal area and occurs on almost all of the plots (Class 3, 5, 7, 9, 43). This level of dominance for a single species is common in Green Ridge's mixed forests, while smaller pockets of forests dominated by 40-50 percent or more relative basal area for a given species occur infrequently (except for white oak) (Class 1, 4, 14, 50). The level of specificity and mixing in our forest alliances probably pushes hyperspectral data to the limits of its current ability to separate spectrally mixed classes using the methods described here.

Nonetheless, it is important to remember that the field validation dataset consists of only one fourth the number of inventory plots used to create the classifications, and these were typically classified correctly at a much higher rate. The learning accuracy reported in Table 2 is more robust in this way because it is derived from a much larger sample size and from the quantitative forest inventory data. The field validation provides an independent assessment of the learning accuracy while also characterizing the fuzzy nature of our forest alliances.

Fuzzy set validation proved extremely useful for validating our satellite based forest maps in the field. It is particularly relevant when mapping a heterogeneous mixed forest with satellite imagery, where the minimum mapping unit is a 17 or 30m^2 pixel. An expert visiting a pixel-sized area on the ground will often find that multiple forest types are acceptable labels for that site. Although the map itself is limited to representing each pixel with only one discrete forest class, much of the forest area is covered by regularly varying mixes of the species that dominate the alliances in Table 1. The canopy reflectance measured for a forest pixel will be a combination of the reflectance from the crowns of all the trees in the pixel area. AVIRIS data samples a smaller area with fewer tree canopies, and thus can be expected to create the most accurate maps, since its pixels experience less spectral mixing than larger pixels.

Sources of Uncertainty

The greatest source of uncertainty for our classification and validation methods was geographic inaccuracy within our AVIRIS image dataset. The AVIRIS data caused the greatest concern because certain distortions in the data caused by the pitch and yaw of the aircraft could not be removed from the data completely. While using hundreds of ground control points created excellent spatial accuracy in most areas, some small regions in the AVIRIS image could be located as far as 80m away from their actual location. This uncertainty inevitably means that some of the spectra sampled from the AVIRIS image to represent certain CFI plots in the CART classification actually sampled the incorrect area. As a result, some proportion of the spectral signatures used to train the classification might have been incorrectly labeled. These problems associated with geographic map errors tend to dampen map learning and validation accuracy values.

We did not account for differences in basal area or forest age with our final classification maps except to mask out areas of recent forest harvests generally characterized by plot basal areas less than 10 m^{2}ha^{-1}. We chose instead to use all the CFI plot data available to map as many classes as possible, though we didn't expect to be able to map classes represented by only one or two CFI plots with good accuracy. Other classification maps were created using only a subset of the data such as plots having a total basal area greater than or equal to 20 m^{2}ha^{-1}. These maps had lower overall accuracy and tended to map forest types to large contiguous areas that probably represented an oversimplification of the mixed forests at Green Ridge. While the forests of Green Ridge are generally even aged, variations in basal area and maturity can introduce variance into the spectral signature bundles representing a given forest type, adding to the difficulty of distinguishing among mixed forest types.

Finally, sources of error are introduced into the dataset from the collection of the field data itself. It has been estimated that forest inventory data may only be about 80 percent accurate, with uncertainty generally coming in the form of misidentified or misrecorded tree species or incorrectly acquired or recorded geographic coordinates.

Conclusions

We were able to map Alliance level forest associations with accuracies generally ranging from 60-90 percent using Hyperspectral imagery from AVIRIS. Hyperion data were more limited in mapping ability, possibly because of its lower signal-to-noise ratio compared to the other data sets (Green et al. 2003) or alternatively because only half as many CFI inventory plots were available for training because of its narrow swath width. Multi-temporal Landsat TM achieved similar accuracy levels as Hyperion but were not as high as AVIRIS. Nevertheless, the ability to map Alliance level forest types with such a high level of accuracy opens up new opportunities to ask and answer questions about the spatial distribution of forest types and to use the information gained to improve forest management.

Acknowledgments

This research was supported by NASA EO-1 Science Validation Team grant NCC5-493. Thanks to Robert Chastain and Brian Sturtevant for their contributions to this work, and to Francis Zumbrun, Chris McCann and the Maryland DNR CFI program for contributing forest data. This paper is Scientific Series Contribution Number 3709, University of Maryland Center of Environmental Science.

Literature Cited

Allen, T. R. 2000. **Topographic normalization of Landsat Thematic Mapper data in three mountain environments.** Geocarto International 15: 13-19.

Cairns, D.M. 2001. **A comparison of methods for predicting vegetation type.** Plant Ecology 156:3-18.

Clark, L. A., and D. Pregibon. 1993. **Tree-based models.** Pages 377-419 in J. M. Chambers and T. J. Hastie, eds., Statistical Models in S. Chapman and Hall, New York, NY.

Czaplewski, R.L. and P.L. Patterson. 2003. **Classification accuracy for stratification with remotely sensed data.** Forest Science 49:402-408.

Friedl, M. A., and C. E. Brodley. 1997. **Decision tree classification of land cover from remotely sensed data.** Remote Sensing of Environment 61: 399-409.

Friedl, M. A., C. E. Brodley, and A. H. Strahler. 1999. **Maximizing land cover classification accuracies produced by decision trees at continental to global scales.** IEEE Transactions on Geoscience and Remote Sensing 37: 969-977.

Gopal, S., and C. Woodcock. 1994. **Theory and methods for accuracy assessment of thematic maps using fuzzy sets.** Photogrammetric Engineering and Remote Sensing 60:181-188.

Green, R. O., B. E. Pavri, and T. G. Chrien. 2003. **On-orbit radiometric and spectral calibration characteristics of EO-1 Hyperion derived with an underflight of AVIRIS and in situ measurements at Salar de Arizaro, Argentina.** IEEE Transactions on Geoscience and Remote Sensing 41:1194-1203.

Hess, L. L., J. M. Melack, S. Filoso, and Y. Wang. 1995. **Delineation of inundated area and vegetation along the Amazon floodplain with the SIR-C synthetic aperture radar.** IEEE Transactions on Geoscience and Remote Sensing 33: 896-904.

Lance, G. N., and W. T. Williams. 1967. **A general theory of classification sorting strategies. I. hierarchical systems.** Computer Journal 9:373-380.

Martin, M. E., S. D. Newman, J. D. Aber, and R. G. Congalton. 1998. **Determining forest species composition using high spectral resolution remote sensing data.** Remote Sensing of Environment 65: 249-254.

Mash, J. 1996. **The land of the living: the story of Maryland's Green Ridge State Forest.** Cumberland, MD: Commercial Press.

Meyer, P., K. I. Itten, T. Kellenberger, S. Sandmeier, and R. Sandmeier. 1993. **Radiometric corrections of topographically induced effects on Landsat TM data in an alpine environment.** ISPRS Journal of Photogrammetry and Remote Sensing 48: 17-28.

Smith, M.L., Martin, M.E., Plourde, L., and S.V. Ollinger. 2003. **Analysis of hyperspectral data for estimation of temperate forest canopy nitrogen concentration: comparison between an airborne (AVIRIS) and a spaceborne (Hyperion) sensor.** IEEE Transactions on Geoscience and Remote Sensing 41:1332-1337.

Townsend, P. A., and S. J. Walsh. 2001. **Remote sensing of forested wetlands: application of multitemporal and multispectral satellite imagery to determine plant community composition and structure in Southeastern USA.** Plant Ecology 157:129-149.

Townsend, P. A., and J. R. Foster. 2002. **Terrain normalization of AVIRIS and Hyperion imagery in forested landscapes.** In R. O. Green, ed., Proceedings of the Eleventh JPL Airborne Earth Science Workshop. JPL, Pasadena, CA.

Townsend, P.A., Foster, J.R., Chastain, R.A., Jr., and W.S. Currie. 2003. **Application of imaging spectroscopy to mapping canopy nitrogen in the forests of the central Appalachian mountains using Hyperion and AVIRIS.** IEEE Transactions on Geoscience and Remote Sensing 41:1347-1354.

Van Aardt, J. A. N., and R. H. Wynne. 2001. **Spectral separability among six southern tree species.** Photogrammetric Engineering and Remote Sensing 67: 1367-1375.

Venables, W. N., and B. D. Ripley. 1994. **Modern Applied Statistics with S-Plus.** Springer-Verlag, New York.